ORIGINAL ARTICLE

Historical biogeography and diversification within the Neotropical parrot genus *Pionopsitta* (Aves: Psittacidae)

Camila C. Ribas[1,2]*, Renato Gaban-Lima[1], Cristina Y. Miyaki[1] and Joel Cracraft[2]

[1]*Instituto de Biociências, Universidade de São Paulo, São Paulo, SP, Brazil and* [2]*Department of Ornithology, American Museum of Natural History, New York, NY, USA*

*Correspondence: Camila Cherem Ribas, Department of Ornithology, American Museum of Natural History, Central Park West at 79th street, New York, NY, USA. 10024.
E-mail: ribas@amnh.org

ABSTRACT

Aim We investigate spatial and temporal patterns of diversification within the Neotropical avifauna using the phylogenetic history of parrots traditionally belonging to the genus *Pionopsitta* Bonaparte 1854. This genus has long been of interest for those studying Neotropical biogeography and diversity, as it encompasses species that occur in most Neotropical forest areas of endemism.

Location The Neotropical lowland forests in South and Central America.

Methods Phylogenetic relationships were investigated for all species of the genus *Pionopsitta* and five other short-tailed parrot genera using complete sequences of the mitochondrial genes cyt *b* and ND2 as well as 26 plumage characters. The resulting phylogeny was used to test the monophyly of the genus, investigate species limits, and as a framework for reconstructing their historical biogeography and patterns of diversification.

Results We found that the genus *Pionopsitta*, as previously defined, is not monophyletic and thus the Chocó, Central American and Amazonian species will now have to be placed in the genus *Gypopsitta*. The molecular and morphological phylogenies are largely congruent, but disagree on the position of one of the Amazon basin taxa. Using molecular sequence data, we estimate that species within *Gypopsitta* diversified between 8.7 and 0.6 Ma, with the main divergences occurring between 3.3 and 6.4 Ma. These temporal results are compared to other taxa showing similar vicariance patterns.

Main conclusions The results suggest that diversification in *Gypopsitta* was influenced mainly by geotectonic events, marine transgressions and river dynamics, whereas Quaternary glacial cycles of forest change seem to have played a minor role in the origination of the currently recognized species.

Keywords
Amazon, biogeography, diversification, *Gypopsitta*, mitochondrial DNA, molecular systematics, parrots, *Pionopsitta*, speciation.

INTRODUCTION

The South American lowlands harbour the richest vertebrate biota on Earth and thus have deservedly attracted considerable interest from those seeking to understand the origin of biological diversity. This region includes tropical wet forests, Amazonian and Atlantic, separated by a belt of more open, drier vegetation – the Chaco, Cerrado and Caatinga. The history of spatial change among these habitats has been proposed as one of the most important causes of diversification in the region (the Pleistocene Refugia hypothesis of Haffer, 1969, 1993, 1997). Other theories and hypotheses to explain the great Neotropical diversity have been primarily ecological (Endler, 1977; Bush, 1994; Tuomisto *et al.*, 1995) or they have invoked landscape changes due to tectonics that lead to isolation and diversification (Wallace, 1852; Platnick & Nelson, 1978; Salo *et al.*, 1986; Cracraft & Prum, 1988). Some of these hypotheses have been tested for some groups (Patton

© 2005 Blackwell Publishing Ltd www.blackwellpublishing.com/jbi doi:10.1111/j.1365-2699.2005.01289.x

et al., 1994), but none is widely accepted, and all workers recognize that different explanations may not be mutually exclusive.

Patterns of diversification and historical biogeography within the lowland Neotropical biota have been investigated in a number of studies, but the history of the region and the processes that originated its great diversity remain poorly understood. Different taxa often show apparent similarities in distributions and areas of endemism, but phylogenetic patterns of the included species frequently reveal that area relationships vary from group to group, with some historical commonality but major differences as well (Cracraft & Prum, 1988; Cracraft, 1988; Aleixo, 2002; Marks *et al.*, 2002; Cortés-Ortiz *et al.*, 2003). At the same time, some authors have attempted to reconstruct the history of the lowland biota using methods that do not rely explicitly on knowledge of phylogenetic relationships, and not unexpectedly these too have revealed similarities and differences in biogeographical pattern (e.g. Bates *et al.*, 1998; Ron, 2000). Nevertheless, a general conclusion that emerges from all these studies – those explicitly phylogenetic and those not – is that the biotic elements (clades) inhabiting the tropical lowlands do not all share a single common pattern but that multiple histories are involved (Cracraft, 1988). Just how those histories might exhibit congruence in spatial vicariance, and what the relative or absolute timing of vicariance events might be are crucial questions that have been the subject of frequent debate. All workers agree, however, that additional phylogenetic studies of groups with species exhibiting congruence in their distributions (i.e. in shared areas of endemism) will be required if the complex evolutionary history of this biota is to be unravelled (e.g. Bates *et al.*, 1998; Marks *et al.*, 2002).

Gypopsitta: an exemplar of Amazonian diversification

Some groups of parrots are especially characteristic of tropical wet forest and have long been of interest to those investigating lowland forest biogeography in that they have species distributed in long-recognized areas of endemism (e.g. Haffer, 1969, 1985; Cracraft, 1985). In particular, parrots in the genus *Gypopsitta* Bonaparte 1856 (traditionally classified in the genus *Pionopsitta* Bonaparte 1854; see below) occur exclusively in forest areas in South and Central America, and their geographically disjunct distributions have made this an especially suitable group for biogeographical inference (Haffer, 1985; Cracraft & Prum, 1988). In this paper, relationships among the eight phylogenetic species of *Gypopsitta* are investigated: one of these, *G. aurantiocephala*, is the most recently described parrot species (Gaban-Lima *et al.*, 2002). In addition to *G. aurantiocephala*, three species – *G. barrabandi* (Kuhl 1820), *G. caica* (Latham 1790) and *G. vulturina* (Kuhl 1820) – are distributed in the Amazon basin, whereas three others – *G. haematotis* (Sclater and Salvin 1860), *G. pulchra* (Berlepsch 1897) and *G. coccinicollaris* (Lawrence 1862) – occur west of the Andes in the forests of north-western South America (Chocó area of endemism) and Central America (Fig. 1). The eighth species, *G. pyrilia* (Bonaparte 1853), occurs in northern South America (Fig. 1). Another species, *Pionopsitta pileata* (Scopoli 1769), formerly thought to be congeneric with these species, is also discussed below.

Cracraft & Prum (1988) undertook the only phylogenetic analysis of the group to date and included all species except the recently described *G. aurantiocephala*. Their findings were based on a cladistic analysis of plumage characters using a species in the genus *Hapalopsittaca* Ridgway 1912 as an outgroup. These authors found that the species included in *Gypopsitta sensu* this paper were grouped into two clades corresponding to taxa distributed east and west of the Andes (Fig. 2). As they noted, knowledge about the spatial and temporal history of *Gypopsitta* (= their *Pionopsitta*) is particularly important because it can provide evidence bearing on several broad questions about the history of the Amazon Basin that have interested numerous investigators (e.g. Haffer, 1967, 1969; Cracraft & Prum, 1988; Bates *et al.*, 1998; Marks *et al.*, 2002; Cortés-Ortiz *et al.*, 2003; Costa, 2003; Aleixo, 2004; Burns & Naoki, 2004): (1) whether *cis*/*trans* (east/west) Andean (i.e. Chocó-Central America and Amazonia) disjunctions are due to orogenic events in the northern Andes or to ecological processes of more recent origin, (2) whether their diversification within the Amazon Basin might be due to climatic oscillations that occurred mainly during the Quaternary, as postulated by the Refugia hypothesis, or to pre-Pleistocene events.

This study was designed to reanalyse the relationships postulated by Cracraft & Prum (1988) using a newly generated molecular data set and broader taxon sampling, and to explore the implications of these data for reconstructing patterns of historical biogeography within the group. We soon discovered, however, that *Pionopsitta* is not monophyletic and that the type species of the genus, *P. pileata*, is phylogenetically distant from the other species. This means that the genus name *Pionopsitta* Bonaparte 1854 is no longer available for the eight remaining species without expanding that genus to include a number of other disparate genera and species. Thus, rather than perpetuate taxonomic confusion by using *Pionopsitta* for a large clade of parrots, a name change was in order. As first revisor, we designate the name *Gypopsitta* Bonaparte 1856, the type species of which is *G. vulturina*, and we accordingly apply *Gypopsitta* to these species throughout this paper. The name *Gypopsitta* is equally as old as other available names, and because it has previously been used for a species in this clade, it maintains a semblance of nomenclatural stability.

MATERIALS AND METHODS

Samples and geographical distribution

Blood and tissue samples were obtained from 29 individuals belonging to *P. pileata* as well as to seven of the eight species of *Gypopsitta*. For the remaining species (*G. pyrilia*), skin samples (toe pads) were obtained from two museum specimens (Table 1, specimens 21 and 22). Skin samples were also

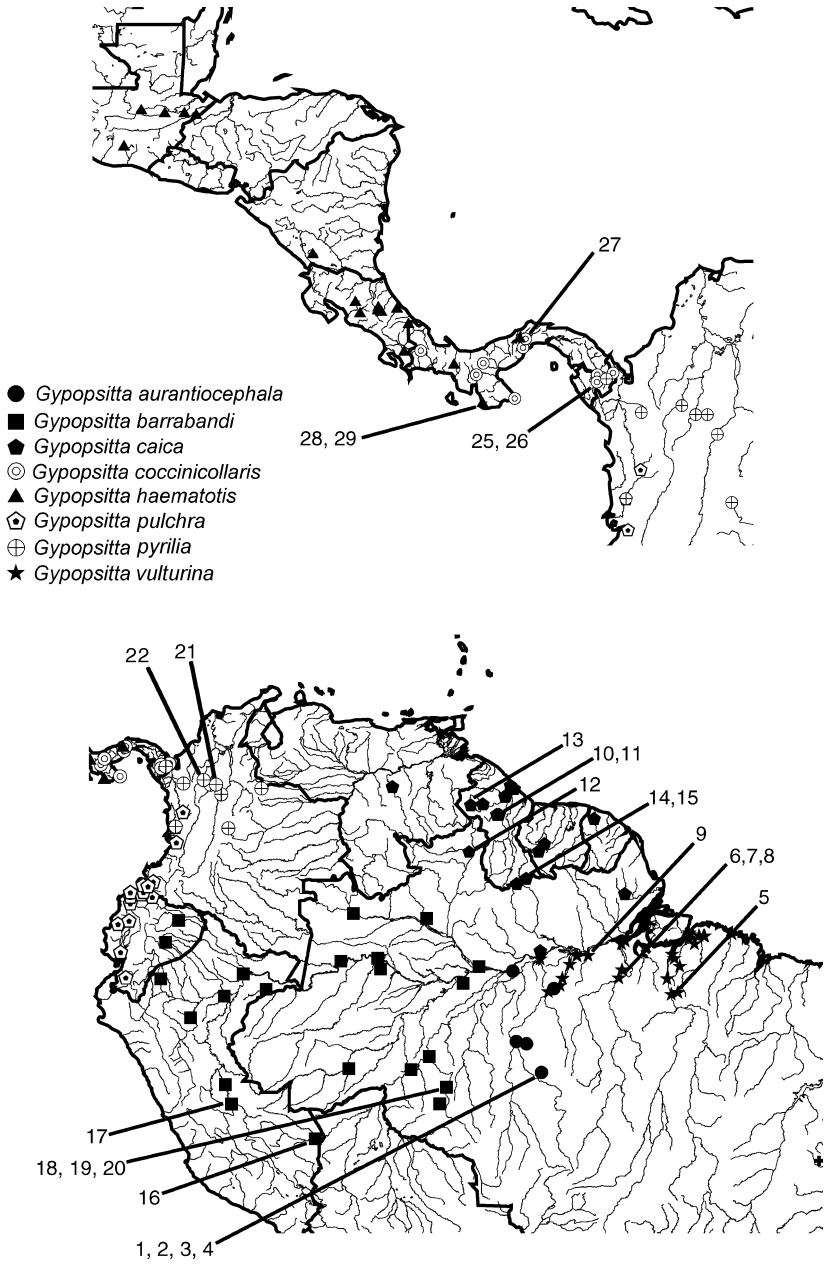

Figure 1 Distribution of species of *Gypopsitta* (determined from locality data obtained from museum collections, see Materials and methods). Numbers correspond to locations of the samples used in this study (see Table 1).

obtained from two individuals of *G. vulturina* (specimens 8 and 9), as only two tissue samples were available. We also used one sample from a formalin-fixed specimen of *G. vulturina* (specimen 5) in order to increase the sampling.

Because the monophyly of *Pionopsitta* (including *Gypopsitta* and *P. pileata*) has not been rigorously tested by molecular data, we included in the analysis seven individuals belonging to closely related genera: *Pionus* Wagler 1832 [*P. menstruus* (Linnaeus 1766) and *P. fuscus* (Müller 1776)], *Graydidascalus* Bonaparte 1854 [*G. brachyurus* (Kuhl 1820)], *Triclaria* Wagler 1832 [*T. malachitacea* (Spix 1824)], *Hapalopsittaca* Ridgway 1912 [*H. amazonina* (Des Murs 1845)] and *Amazona* Lesson 1830 [*A. xanthops* (Spix 1824)] (but see Russello & Amato, 2003). Three individuals belonging to three different genera of more distantly related 'long-tailed' parrots, *Pyrrhura picta* (Müller 1776), *Aratinga weddelli* (Deville 1851) and *Anodorhynchus leari* Bonaparte 1856 (see Miyaki *et al.*, 1998; Ribas & Miyaki, 2004; Tavares *et al.*, 2004), were also included as distant outgroups.

Collection locality records for all species belonging to the genus *Gypopsitta* were gathered from museum collections (Museu de Zoologia da Universidade de São Paulo, Museu Nacional do Rio de Janeiro, American Museum of Natural History, Yale Peabody Museum of Natural History, Field Museum of Natural History and Museum of Vertebrate Zoology, Berkeley) in order to construct the distribution map shown in Fig. 1. Localities corresponding to individuals included in this study are given in Table 1.

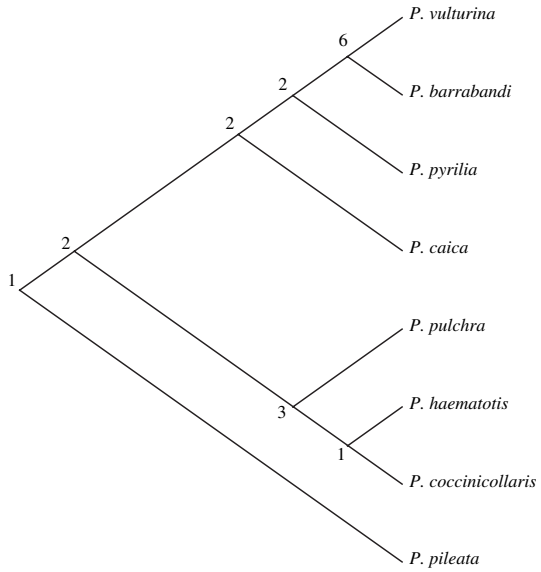

Figure 2 Relationships among species of *Gypopsitta* (= *Pionopsitta*) found by Cracraft & Prum (1988) based on 26 plumage characters. The tree has 29 steps: the number of character changes supporting each node is shown.

DNA extraction, amplification and sequencing

DNA extraction from blood samples was performed through incubation of a small amount of blood at 54 °C with proteinase K for *c.* 4 h followed by the phenol-chloroform procedure. Extraction from tissue, skin and formalin-fixed tissue samples was performed using the DNeasy tissue kit (Qiagen, Valencia, CA, USA) following the manufacturer's recommendations. Samples were incubated in proteinase K for 4 h for tissues and overnight for skin and formalin-fixed samples. DTT was added to the incubation buffer for all samples. Formalin-fixed tissue samples were extensively washed in sterile water prior to extraction. All the materials used for handling the skin and formalin-fixed tissue samples were irradiated with ultraviolet light prior to use and extra care was taken to avoid contamination. Negative controls were used during all procedures.

The entire genes that code for cytochrome *b* (hereafter cyt *b*) and for the subunit 2 of the NADH dehydrogenase (ND2) were sequenced for all samples. Sequencing two separate genes allowed us to compare the patterns of sequence evolution in this avian group and to assess the utility of each gene in resolving relationships at different phylogenetic levels. DNA extracted from fresh tissue and blood samples was amplified using 40 μL reaction volumes containing: 2.0 μL DNA solution, 1x PCR buffer (Promega, Madison, WI, USA), 2.5 mM $MgCl_2$, 0.8 mM dNTPs, 0.5 μM of each primer and 2 U of Taq DNA polymerase (Promega). DNA extracted from skin and formalin-fixed tissue samples was amplified in 40 μL reaction volumes containing: 2.0 μL DNA solution, 1x PCR buffer (Qiagen), 1 mM sterile dNTPs (Takara Biomedicals, OTSU, Shiga, JP), 1 μM of each primer and 1 U of HotStarTaq DNA polymerase (Qiagen). Primer sequences are shown in Table 2.

Amplifications of the entire genes (cyt *b* and ND2) using external primers were performed and the products of these reactions were visualized by electrophoresis in 1.3% low-melting-agarose gels run in TAE (Tris-acetate low-EDTA buffer, pH 7.8). The single amplification products were cut, dissolved in 200 μL of sterile water, heated at 70 °C for 15 min and stored at room temperature. These products were then used as templates for a re-amplification reaction using internal primers, under the same conditions described above, but with higher annealing temperatures.

For amplification from DNA extracted from skins and from formalin-fixed tissues, reactions were performed using six pairs of primers for each gene (Table 2) designed to amplify fragments of *c.* 250 base pairs (bp) with overlap of at least 50 bp between adjacent fragments.

Amplification products were visualized through electrophoresis in agarose gels. Purification of products was performed with the QIAquick 96 PCR BioRobot kit (Qiagen) using the BioRobot 9600 (Qiagen). One to three microlitres of the purified PCR product were used as template for the 11 μL sequencing reaction using dRhod (Applied Biosystems, Foster City, CA, USA). Sequencing primers were the same used for the amplifications and re-amplifications. Ethanol precipitation of the cycle sequencing product was performed and the samples were run on a 3100 Automated DNA Sequencer following the ABI protocol.

Sequence alignment and analysis

Chromatograms were edited, aligned and confirmed using Sequencher 4.1 (Gene Codes Corporation, Ann Arbor, MI, USA). Nucleotide sequences were determined by comparing the heavy and light strands and visually checked for miscalls. The alignment was performed manually using MacClade 4.0 (Maddison & Maddison, 1999) and sequences were translated to confirm the correct reading frame positions and to check for the presence of stop codons.

MEGA (Kumar *et al.*, 2001) was used to calculate *p*-distances (Nei, 1987) and standard errors within and among taxa. Maximum likelihood (ML) distances using parameters selected by MODELTEST (Posada & Crandall, 1998) were calculated using PAUP*4.0b10 (Swofford, 1998). The number of transition and transversion substitutions at each codon position was plotted against *p*-distances to test for evidence of saturation due to multiple substitutions in the two genes. Evolutionary rates in the two genes were compared by plotting pairwise percentage sequence divergences in cyt *b* against those in ND2. To determine if cyt *b* and ND2 contain similar phylogenetic signal, phylogenetic congruence was evaluated via the partition homogeneity test (Farris *et al.*, 1995) with 100 replicates in PAUP* and also through comparison of separate analyses of the two data sets. Another partition homogeneity test compared the three codon positions. The uniformity of base composition at each codon

Table 1 Taxa, identification number in the present study, collection numbers, institutions and collection locality

Taxon	No.	Voucher	Institution*	Collection locality
Gypopsitta aurantiocephala	1	3668	USP	Cururu River, Jacareacanga, Para, Brazil
Gypopsitta aurantiocephala	2	2943	USP	Cururu River, Jacareacanga, Para, Brazil
Gypopsitta aurantiocephala	3	2944	USP	Cururu River, Jacareacanga, Para, Brazil
Gypopsitta aurantiocephala	4	2949	USP	Cururu River, Jacareacanga, Para, Brazil
Gypopsitta vulturina	5	A4955	MPEG	Tocantins River, Sacunda, Para, Brazil
Gypopsitta vulturina	6	B6888	NMNH	Xingu River, Altamira, Para, Brazil
Gypopsitta vulturina	7	B6905	NMNH	Xingu River, Altamira, Para, Brazil
Gypopsitta vulturina	8	429164	AMNH	Xingu River, Para, Brazil
Gypopsitta vulturina	9	288269	AMNH	Limoatuba, Tapajos River, Para, Brazil
Gypopsitta caica	10	7587	ANSP	Iwokrama Reserve, Guyana
Gypopsitta caica	11	7638	ANSP	Iwokrama Reserve, Guyana
Gypopsitta caica	12	389173	FMNH	Branco River, Boa Vista, Roraima, Brazil
Gypopsitta caica	13	B09175	NMNH	North-western Baramita, Guyana
Gypopsitta caica	14	B11726	NMNH	Upper Essequibo River, Guyana
Gypopsitta caica	15	B10779	NMNH	Acari Mountains, Guyana
Gypopsitta barrabandi	16	B9596	LSUMNS	Nicolas Suarez, Pando Department, Bolivia
Gypopsitta barrabandi	17	B10823	LSUMNS	Shesha River, Pando Department, Peru
Gypopsitta barrabandi	18	389690	FMNH	Jiparana River, Rondonia, Brazil
Gypopsitta barrabandi	19	389691	FMNH	Jiparana River, Rondonia, Brazil
Gypopsitta barrabandi	20	389693	FMNH	Jiparana River, Rondonia, Brazil
Gypopsitta pyrilia	21	475573	AMNH	Remedios, South-western Colombia
Gypopsitta pyrilia	22	133049	AMNH	Cauca River, Puerto Valdivia, Colombia
Gypopsitta pulchra	23	B1448	LSUMNS	Zoo/Captive
Gypopsitta pulchra	24	B1449	LSUMNS	Zoo/Captive
Gypopsitta coccinicollaris	25	B2185	LSUMNS	Cerro Pire, Darien Province, Panama
Gypopsitta coccinicollaris	26	B2201	LSUMNS	Cerro Pire, Darien Province, Panama
Gypopsitta coccinicollaris	27	B26852	LSUMNS	Gamboa, Colon Province, Panama
Gypopsitta haematotis	28	5769	ANSP	Cascajilloso, Veraguas, Panama
Gypopsitta haematotis	29	5770	ANSP	Cascajilloso, Veraguas, Panama
Pionopsitta pileata	30	494/SOBf396	USP	Captive
Pionopsitta pileata	31	3466	USP	Captive/Sorocaba Zoo
Pionopsitta pileata	32	3467	USP	Captive
Pionopsitta pileata	33	3850/SOB96787	USP	Captive
Pionopsitta pileata	34	3851/SOB97484	USP	Captive
Pionus menstruus	35	2087	USP	Acre, Brazil
Pionus fuscus	36	5017	KUMNH	Guyana
Graydidascalus brachyurus	37	1623	USP	Rio Busutuba, Ilha Caviana, Pará, Brazil
Graydidascalus brachyurus	38	286592	FMNH	Loreto, Peru
Amazona xanthops	39	1876	USP	Captive
Hapalopsittaca amazonina	40	32099	LSU	Cajamarca Department, Peru
Triclaria malachitacea	41	415	USP	Captive
Aratinga weddelli	42	2085	USP	Acre, Brazil
Pyrrhura picta	43	5039	NMNH	Baramita, Guyana
Anodorhynchus leari	44	410	USP	Captive

*USP, Universidade de São Paulo; MPEG, Museu Paraense Emílio Goeldi; NMNH, National Museum of Natural History; AMNH, American Museum of Natural History; ANSP, Academy of Natural Sciences of Philadelphia; FMNH, Field Museum of Natural History; LSUMNS, Louisiana State University Museum of Natural History; KUMNH, Kansas University Museum of Natural History.

position was evaluated through a chi-square test of homogeneity.

Phylogenetic analysis was undertaken for each gene independently (cyt *b*, 1140 bp and ND2, 1041 bp) and in combination (2181 bp), employing maximum parsimony (MP) and ML using PAUP* as well as with Bayesian analysis using MrBayes v3.0 b4 (Huelsenbeck & Ronquist, 2001).

MP analyses were implemented with heuristic tree searches, tree bisection reconnection (TBR) branch swapping, and 100 random addition sequence replications. Searches were performed using equally weighted characters and including all substitutions. The relative support for inferred monophyletic groupings was determined using 1000 bootstrap replications and decay indices (Bremer, 1994) calculated with Autodecay

Table 2 Primers used to amplify cyt *b* and ND2

Gene	Primers	Sequence 5′–3′	Reference
Cyt *b* (tissues)	N5L14750	GGACCAGAAGGACTTGCCGACCTA	This paper
	CBH15422	GGTGGGGTTGTCTACGGAGAA	This paper
	CBL 15298	TGAGGCCAAATATCATTCTGAGGGGC	Cheng *et al.* (1994)
	CBH 15764	CCTCCTAGTTTGTTGGGGATTGA	Miyaki *et al.* (1998)
	CBL 15507	AACCTACTAGGAGACCCAGA	J. Feinstein (pers. comm.)
	HB20	TTGGTTCACAAGACCAATGTT	J. Feinstein (pers. comm.)
Cyt *b* (skins and formalin-fixed tissue)	N5L 14839	GATCGTTCGCACTATCCACCC	This paper
	CBH 15120	GGAGGTTGCGGATTAGTCAACCG	
	CBL 15062	CTGCAGACACCTCCCTAGCC	
	CBH 15315	GTGATAACTGTGGCTCCTCAG	
	CBL 15249	CCTCCTACTCACCCTCATAGC	
	CBH 15516	TTAGATGAAATGCCTAGGGGG	
	CBL 15462	CACCAGCCTAGTCCTCGTCC	
	CBH 15708	GCGTATGCGAATAGGAAGTATCAT	
	CBL 15660	CTTCACCCCAGCAAACCCCCTAG	
	CBH 15902	ACTGGTTGACTTCCTACTCATG	
	CBL 15845	TCCGCCCCGCCTCACAACTCC	
	ThrH 16058	GTTCACAAGACCAATGTT	
ND2 (tissues)	LMet	GGCCCATACCCCGAAAATGA	J. Groth (pers. comm.)
	H5764	GAGAAGCTAGGATTTTTCGTG	P. Brito (pers. comm.)
	L5602	GATTCCCAGAAGTTCTTCAAGG	P. Brito (pers. comm.)
	H6313	CTCTTATTTAAGGCTTTGAAGGC	Sorenson *et al.* (1999)
ND2 (skins and formalin-fixed tissue)	Met L5215	TGATGGTTCAACCCCTTCCCT	This paper
	H5485	CCTGTGTGTTGTGCGTTGATTGTGC	
	L5394	GCCATTGAAGCAGCAACCAAATA	
	H5636	TGTTGAAAGGAGTATGGCAGT	
	L5574	CACTTTTGATTTCCAGAAGTACTTC	
	H5823	CAATGGTGATTATTATTCA	
	L5745	GGATTAAACCAAACACAAACACG	
	H6005	AGGGAGGCCCGATAATGATAG	
	L5932	TAACCTCATGAACCAAGGCCCC	
	H6180	GCTTTATTTTGCCTGAGGGGTT	
	L6108	CTGTTCTTCTACCTACGCCTAGC	
	Trp H6313	GAAGGCCTTTGGTTTGTGTTATCCTAAG	

version 4.0 (Eriksson, 1999; 100 random-addition replicates per tree).

The likelihood ratio test as implemented in MODELTEST (Posada & Crandall, 1998) was used to select the simplest model of molecular evolution yielding a significantly higher likelihood than others. The model selected was used for the ML analyses, which were implemented using heuristic tree search, TBR branch swapping and 10 random addition replicates. Branch support on the ML tree was assessed by 100 bootstrap replications using a starting tree obtained by neighbour-joining and SPR (subTree proning-regrafting) branch swapping. In order to understand better the sensitivity of data to the different ML parameters, Bayesian inference of phylogeny was implemented using MrBayes v3.0 b4 (Huelsenbeck & Ronquist, 2001). Following the ML models that were selected by MODELTEST for each data set (cyt *b* and ND2), we chose a GTR + I + Γ model of sequence evolution. The analysis was run using partitioned likelihood, so that the parameters could vary independently for the two genes in the combined analysis. Four simultaneous chains were run for 1,000,000 generations with trees being sampled every 100 generations for a total of 10,000 trees. The ML scores became stable (stopped improving) around the 1000th tree, so that burn-in was completed by the 1000th tree, and 9000 trees were kept in each analysis. Three independent analyses were performed for the combined data set and the 27,000 sampled trees were used to compute the posterior probabilities of each node.

Morphological analysis

External character variation among the species of *Gypopsitta* was analysed using specimens housed in the American Museum of Natural History (New York). As described below, the tree was rooted using outgroup comparison. The characters defined previously by Cracraft & Prum (1988) were re-examined and scored again, and some were discarded and new ones were added to the analysis. The character matrix was

constructed in MacClade 4.0 and analysed in PAUP* using MP with unordered characters.

Tests for comparisons of different topologies

Different tests have been proposed to compare a topology obtained in a phylogenetic analysis with another topology derived from a different data set or different method of phylogenetic reconstruction. Templeton's test (Templeton, 1983) and the Kishino–Hasegawa test (Kishino & Hasegawa, 1989) were the first ones used for this purpose, but both have been criticized as being inappropriate for comparing trees that have not been defined *a priori* (Goldman *et al.*, 2000). Alternative tests that have been proposed include the Shimodaira–Hasegawa test (Shimodaira & Hasegawa, 1999), the SOWH test (Goldman *et al.*, 2000), and the parametric bootstrap test (Huelsenbeck *et al.*, 1996), and we used these to compare the topologies obtained in the molecular and morphological analyses. All three tests were performed using a reduced molecular data set containing only one representative of each species of *Gypopsitta* and two outgroups (matrix with 11 taxa, 2181 bp), with the morphological topology being used as the null hypothesis. Analysis of the reduced data set resulted in the same relationships among taxa as were found using all individuals.

The Shimodaira–Hasegawa test was performed in PAUP*. The SOWH test was performed following the protocol suggested by Anderson, Goldman and Rodrigo (Guidelines for performing the SOWH test, http://www.ebi.ac.uk/goldman/tests/SOWHinstr.html): 100 simulated data sets were generated via parametric bootstraping (REV, GTR model) using the program Seq-Gen 1.2.6 (Rambaut & Grassly, 1997); for each simulated data set the ML topology was obtained and its log likelihood compared to the log likelihood of the null hypothesis (the topology obtained from morphological data). The distribution of the differences in log likelihood was used to determine the null distribution for a one-tailed test at a significance level of 5% (Goldman *et al.*, 2000). The test was performed with full optimization, using the reduced data set, TBR branch swapping, and with a starting tree obtained by neighbour-joining. For the parametric bootstrap test, another set of simulated data sets was obtained using Seq-Gen 1.2.6 (REV, GTR) with parameters estimated from the ML topology. The differences in length between the trees obtained from each data set and the null hypothesis were used to determine the null distribution, and a one-tailed test at a significance level of 5% was used to test for the rejection of the null hypothesis.

Molecular dating of divergence times

A likelihood ratio test assuming a chi-square distribution with number of taxa minus two degrees of freedom (Huelsenbeck & Rannala, 1997) was applied to the cyt *b*, ND2, and combined matrices containing only the species belonging to *Gypopsitta* and *H. amazonina* as outgroup (see Results) in order to compare the log-likelihood values from ML trees constructed with or without a molecular clock constraint. In addition, branch length and two cluster tests were applied to these matrices using Lintree (Takezaki *et al.*, 1995).

The absence of a reliable psittacid fossil record or geological calibration point prevents a calculable estimate of a local substitution rate. As an alternative solution, a range of divergence times was estimated using the branch lengths of the ML tree and applying substitution rates that have been estimated for other bird species (see below). Branch lengths and standard errors for the ML tree were calculated using Lintree (Takezaki *et al.*, 1995). Two different rates of cyt *b* sequence divergence were used, one based on a geological calibration of island formation (1.6% Myr^{-1}, Fleischer *et al.*, 1998) and the other locally calibrated for other bird species using fossil records (2.0% Myr^{-1}, Shields & Wilson, 1987; Randi, 1996).

RESULTS

Molecular characterization

Sequences from the entire cyt *b* (1140 bp) and ND2 (1041) genes were obtained for all individuals studied (GenBank accession numbers: AY669400–AY669487). All sequences were easily aligned manually and no indels were present. Gene sequences began with the ATG (cyt *b*) or ATA (ND2) start codons and both terminated with TAA stop codon for all individuals. Although nuclear copies of mitochondrial genes in birds have been reported before (Quinn, 1997), there is evidence that we have sequenced functional mtDNA genes: (1) we performed long amplifications of both genes for most individuals studied; (2) when using internal primers to perform the amplifications from skin and formalin-fixed tissue samples, we utilized specially designed, and very specific, primers; we sequenced fragments that overlapped by at least 50 bp and found no ambiguities or differences in these regions; (3) there were no unexpected stop codons; (4) no contaminants were detected in the PCR products; and (5) all sequences obtained aligned easily to other psittacine mitochondrial sequences.

Variable and parsimony informative sites, base composition and transition/transversion (Ti/Tv) ratios are shown for each gene and for the combined data in Table 3. Base composition analyses showed a higher frequency of adenine and cytosine in both genes, mainly at third positions (Table 3). No base composition bias was detected among taxa in the data sets, including variable sites only ($P = 0.99$ for cyt *b* and $P = 0.72$ for ND2), and considering each codon position independently ($P = 1$ for first and second positions in cyt *b* and ND2; $P = 0.96$ for third position in cyt *b* and $P = 0.54$ for third position in ND2). The results of the partition homogeneity test (Farris *et al.*, 1995) on the combined data set revealed significant congruence between genes ($P = 0.53$) and also among codon positions for both genes ($P = 0.91$ for ND2 and $P = 0.72$ for cyt *b*).

Table 3 Variable and informative sites and base composition for each gene and for the combined data set

Gene	Cyt *b*	ND2	Combined
Number of base pairs	1140	1041	2181
Number of individuals	44	44	44
Variable first/second/third	108/32/314	141/78/287	249/110/601
Informative first/second/third	82/18/269	104/50/235	186/68/504
%A first/second/third	0.266/0.204/0.378	0.391/0.161/0.419	0.325/0.184/0.397
%C first/second/third	0.289/0.280/0.480	0.280/0.368/0.407	0.285/0.322/0.445
%G first/second/third	0.205/0.127/0.044	0.132/0.089/0.046	0.170/0.109/0.045
%T first/second/third	0.239/0.388/0.098	0.197/0.381/0.127	0.219/0.385/0.112
Ti/Tv ratio	9.95	6.53	7.85
rAC	1.0822	0.3295	0.5167
rAG	24.6281	11.0585	16.3688
rAT	1.2988	0.3012	0.5076
rCG	0.3497	0.2059	0.2328
rCT	24.6281	4.6667	8.1367
α	1.9249	1.5953	1.8819
pinv	0.5417	0.4067	0.4838
Tree length (ML)	1.64	1.89	2.79
−ln L	6627.3698	6688.57024	7290.31981
No. trees (MP)	12	36	3
Tree length (MP)	1123	1172	1578

Comparisons of pairwise distances between the two genes showed a similar pattern of rates of sequence divergence, with cyt *b* evolving slower than ND2 at divergence levels *c.* > 5% (overall slope 0.667) (Fig. 3). All transversion substitutions (data not shown) and transition substitutions at first and second positions increased linearly with percentage sequence divergence in both genes (Fig. 3). Third position transitions showed evidence of multiple hits only when sequences from other genera (other than *Gypopsitta*) were included in the comparisons (Fig. 3). Multiple hits in cyt *b* were evident at levels of sequence divergence above 8% and in ND2 multiple hits occurred only above 12% divergence.

For the measures of uncorrected pairwise sequence divergence, individuals belonging to each taxon were grouped and the distances and standard errors were measured within and between groups (Tables 4 and 5). Intra-specific divergence ranged from 0.1% to 1.2% while inter-specific divergences ranged from 1% to 16% (excluding the long-tailed outgroups). Distances between *Gypopsitta* species and *P. pileata* ranged from 10.8% to 11.9% in cyt *b* and from 15.1% to 16.0% in ND2 sequences. Comparisons among *Gypopsitta* species never exceeded 8.1% in cyt *b* and 10.9% in ND2.

The smallest inter-specific genetic distances were found between individuals of *G. vulturina* and *G. aurantiocephala* (1.0% in cyt *b* and 1.5% in ND2). There were 20 variable sites in the cyt *b* sequences of individuals of *G. aurantiocephala* ($n = 4$) and *G. vulturina* ($n = 5$). Of these 20, only two were exclusive to *G. vulturina* and thus diagnostic, whereas five were diagnostic for *G. aurantiocephala*. There was one amino acid replacement (position 199) that was exclusive to all individuals of *G. aurantiocephala*. In the ND2 sequences, there were 28 variable sites, with six being diagnostic for each species. There were also two amino acid differences (positions 91 and 310) exclusive to *G. aurantiocephala* and one (position 193) exclusive to *G. vulturina*.

Phylogenetic analyses

Independent MP analyses with all characters unweighted were performed on 44 terminals for cyt *b* (1140 bp), ND2 (1041 bp), and the combined data set (2181 bp). These analyses resulted in 12 most-parsimonious trees for the cyt *b* data, 36 trees for ND2, and three trees for the combined analysis (see Table 3 for trees characteristics). Within each data set trees were congruent, with the only differences being in the relationships among individuals of the same species-level taxon. Topologies obtained for the three different data sets were also largely congruent, the only difference being a basal polytomy when cyt *b* data were analysed independently. The topology found for the combined data is shown in Fig. 4, along with bootstrap values (1000 replicates using heuristic searches) and decay indices (Bremer, 1994). *Hapalopsittaca amazonina* is the sister group to the eight *Gypopsitta* species with high support. This clade, in turn, appears as sister to the *Pionus*/*Graydidascalus*/*Amazona* clade but with low support, and *P. pileata*, is sister to *Triclaria malachitacea*.

The results from MODELTEST indicated that the most complex model of sequence evolution (general time reversible with a proportion of invariant sites and rates at variable sites following a Γ frequency distribution, GTR + I + Γ) offered a significant increase in likelihood over less complex models for all three data sets (details in Table 3). ML analyses of each data set resulted in similar topologies, the only difference, again, was a basal polytomy in the cyt *b* analysis. The topology found in the combined analysis is shown in Fig. 5, along with ML bootstrap values and Bayesian posterior probabilities as

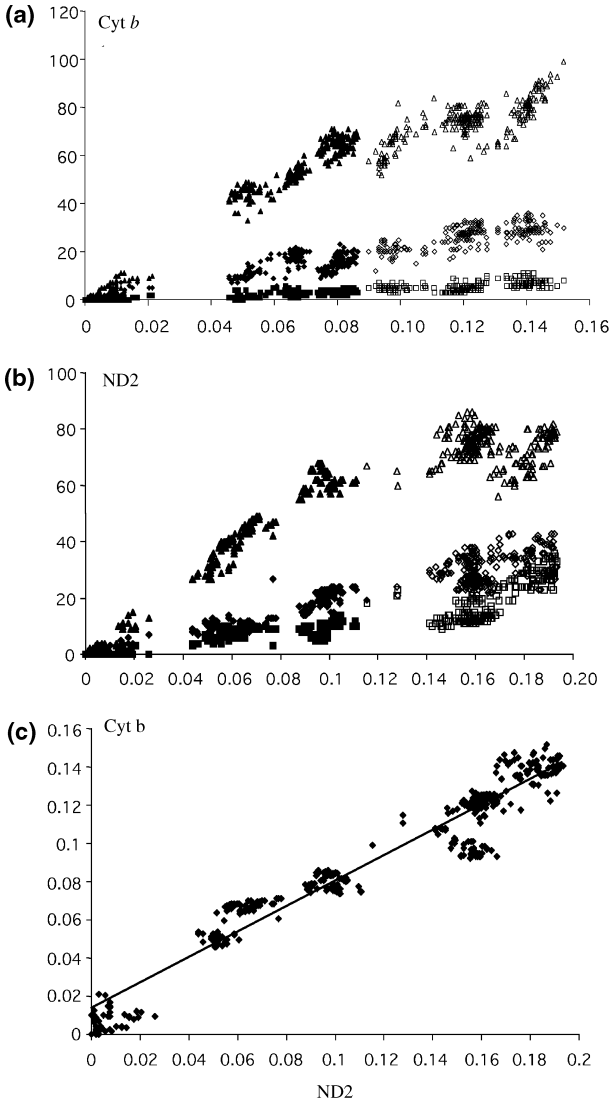

Figure 3 Saturation analyses. (a, b) Pairwise transition sequence distance (absolute number of changes) plotted against total sequence distance (*p*-distance) for first (diamonds), second (squares) and third (triangles) codon positions for cytochrome *b* and ND2. Solid symbols indicate comparisons inside *Gypopsitta*. (c) Pairwise *p*-distances for cytochrome *b* plotted against those for ND2.

measures of support. Both ML and Bayesian analyses found the same topology, and those were nearly congruent with that found using MP, the only difference being that in MP *T. malachitacea* groups with *P. pileata*, while in ML analysis this does not happen (Fig. 4). The relationships among the species of *Gypopsitta* were the same in all analyses.

All analyses discovered the non-monophyly of the genus *Pionopsitta* as defined in the traditional taxonomy. *Hapalopsittaca* groups with the eight *Gypopsitta* species with high support. The node uniting *Gypopsitta* and *Hapalopsittaca* with the clade composed of *Pionus*, *Graydidascalus* and *Amazona* had low support in all analyses. The node uniting all these taxa to *Triclaria* had high support in ML and Bayesian analyses. *Pionopsitta pileata* always appeared in a basal position. Also, in all analyses, *Gypopsitta* was divided into two well-supported clades showing strong *cis*/*trans* Andean distributions (see below).

Table 4 *p*-distances within groups of individuals belonging to the same taxon

		p-distance (SE)	
	n	Cyt *b*	ND2
G. aurantiocephala	4	0.002 (0.001)	0.001 (0.001)
G. vulturina	5	0.003 (0.001)	0.005 (0.001)
G. caica	6	0.004 (0.001)	0.008 (0.002)
G. barrabandi	5	0.008 (0.002)	0.004 (0.001)
G. pyrilia	2	0.007 (0.003)	0.003 (0.002)
G. pulchra	2	0.010 (0.003)	0.005 (0.002)
G. coccinicollaris	3	0.012 (0.003)	0.001 (0.001)
G. haematotis	2	0.009 (0.003)	0.003 (0.002)
P. pileata	5	0.005 (0.002)	0.001 (0.001)

n, Number of individuals; SE, standard error.

Morphological analysis

The relationships revealed by the new molecular data (Figs 4 & 5) are not entirely congruent with those proposed by Cracraft & Prum (1988) on the basis of morphology (Fig. 2), especially among the species taxa of the Amazon basin. In the 1988 morphological analysis of Cracraft & Prum, however, relationships within *Pionopsitta* were examined assuming that the genus as traditionally defined (including *P. pileata*) was monophyletic. *Hapalopsittaca melanotis* was then used to root that tree. As in the present molecular analyses, that morphological analysis found *P. pileata* to lie outside the other species, which were divided into two major *cis*/*trans* Andean clades. Because the molecular data strongly support removing *P. pileata* from the genus, it is possible that morphological character optimizations in the original study were compromised due to the assumption of *Pionopsitta* monophyly. We therefore undertook a new analysis of the morphological data in order to understand better phenotypic evolution within *Gypopsitta* (see Table 6).

Morphological comparisons using a range of taxa included in the molecular analyses (Figs 4 & 5) supported the hypothesis that *Hapalopsittaca* is closely related to *Gypopsitta*. Thus, the two genera share a number of characters not generally found in the other distantly related genera used in the molecular analysis, including: (1) a diffuse upper breast patch that is green and tinged brownish or yellowish, (2) under-tail coverts that have lost red pigment, (3) the loss of a strong, distinct notch along the edge of upper mandible, and (4) the loss of dark blue feathers on the upper breast and/or belly. Although additional work on generic interrelationships will be necessary using increased taxon sampling, molecular and

Table 5 *p*-distance among groups of individuals belonging to different taxa, cyt *b* below diagonal, ND2 above

	1	2	3	4	5	6	7	8	9	10	11	12	13	14	15
1 *G. aurantiocephala*	–	0.015	0.043	0.055	0.063	0.095	0.098	0.103	0.155	0.150	0.148	141	0.152	0.148	0.177
2 *G. vulturina*	0.010	–	0.045	0.056	0.063	0.093	0.095	0.103	0.153	0.151	0.150	0.141	0.148	0.151	0.181
3 *G. caica*	0.047	0.042	–	0.064	0.070	0.092	0.097	0.106	0.152	0.148	0.146	0.141	0.151	0.144	0.178
4 *G. barrabandi*	0.061	0.058	0.063	–	0.048	0.094	0.092	0.099	0.151	0.146	0.149	0.146	0.154	0.140	0.175
5 *G. pyrilia*	0.049	0.050	0.066	0.058	–	0.105	0.101	0.109	0.160	0.139	0.148	0.142	0.149	0.145	0.180
6 *G. pulchra*	0.071	0.071	0.072	0.081	0.080	–	0.052	0.059	0.155	0.144	0.141	0.137	0.148	0.151	0.177
7 *G. coccinicollaris*	0.071	0.071	0.067	0.074	0.075	0.048	–	0.026	0.153	0.142	0.137	0.135	0.136	0.150	0.180
8 *G. haematotis*	0.069	0.070	0.071	0.077	0.073	0.061	0.046	–	0.156	0.146	0.145	0.139	0.141	0.151	0.180
9 *P. pileata*	0.116	0.116	0.112	0.118	0.112	0.119	0.108	0.110	–	0.140	0.165	0.123	0.142	0.140	0.169
10 *Pionus*	0.090	0.090	0.087	0.093	0.092	0.098	0.087	0.087	0.105	–	0.141	0.097	0.124	0.130	0.157
11 *Hapalopsittaca*	0.114	0.115	0.109	0.108	0.115	0.114	0.111	0.107	0.138	0.110	–	0.142	0.150	0.161	0.183
12 *Graydidascalus*	0.107	0.106	0.107	0.112	0.109	0.116	0.110	0.102	0.125	0.103	0.135	–	0.083	0.111	0.147
13 *Amazona*	0.098	0.096	0.094	0.108	0.105	0.111	0.099	0.096	0.116	0.080	0.122	0.090	–	0.129	0.164
14 *Triclaria*	0.106	0.106	0.105	0.105	0.105	0.114	0.108	0.098	0.110	0.095	0.120	0.103	0.097	–	0.160
15 Outgroups	0.127	0.126	0.123	0.124	0.125	0.142	0.124	0.127	0.130	0.110	0.145	0.135	0.122	0.129	–

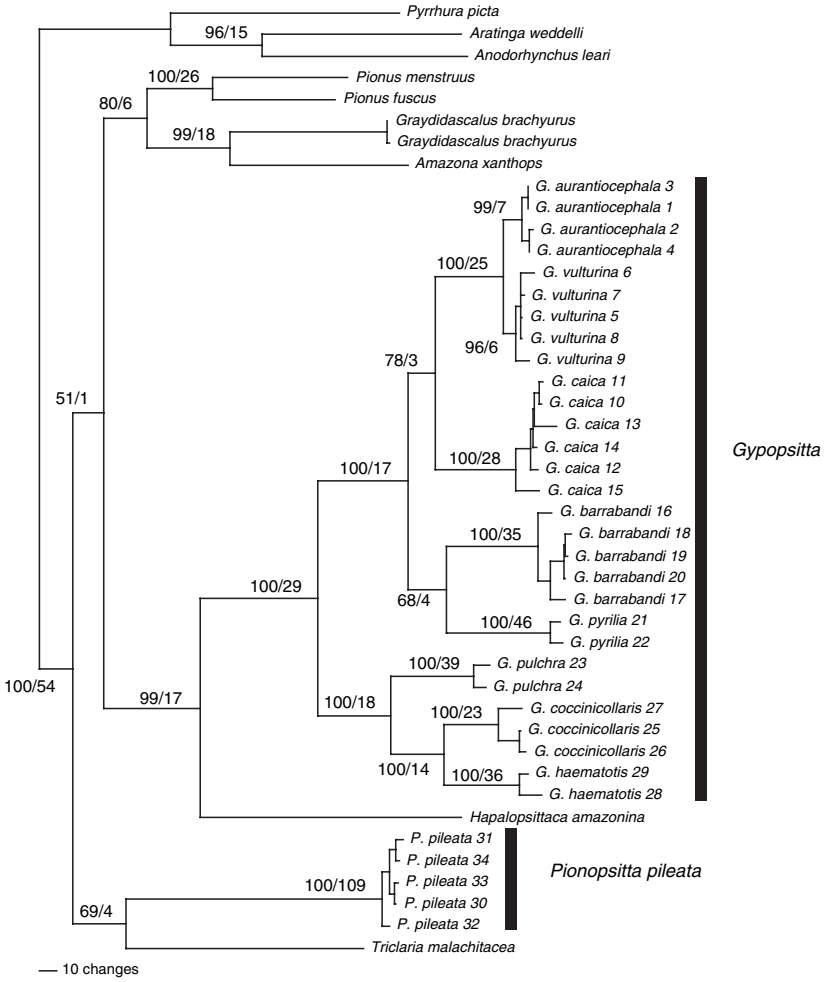

Figure 4 Maximum parsimony analysis of combined data (2181 bp): one of the three topologies found in PAUP. MP bootstrap proportions and decay indices, respectively, are shown on nodes.

morphological data currently available support the hypothesis that *Hapalopsittaca* is the likely sister group to *Gypopsitta* and therefore is an appropriate outgroup taxon.

Twenty-six plumage characters were scored for *H. amazonina* and the eight taxa of *Gypopsitta* (Table 6). *Hapalopsittaca amazonina* was included instead of *H. melanotis*, which was used originally by Cracraft & Prum (1988), because tissue samples for DNA analysis were only available for the former species. Phylogenetic analysis was conducted using MP implemented in PAUP* and the resulting topology is shown in

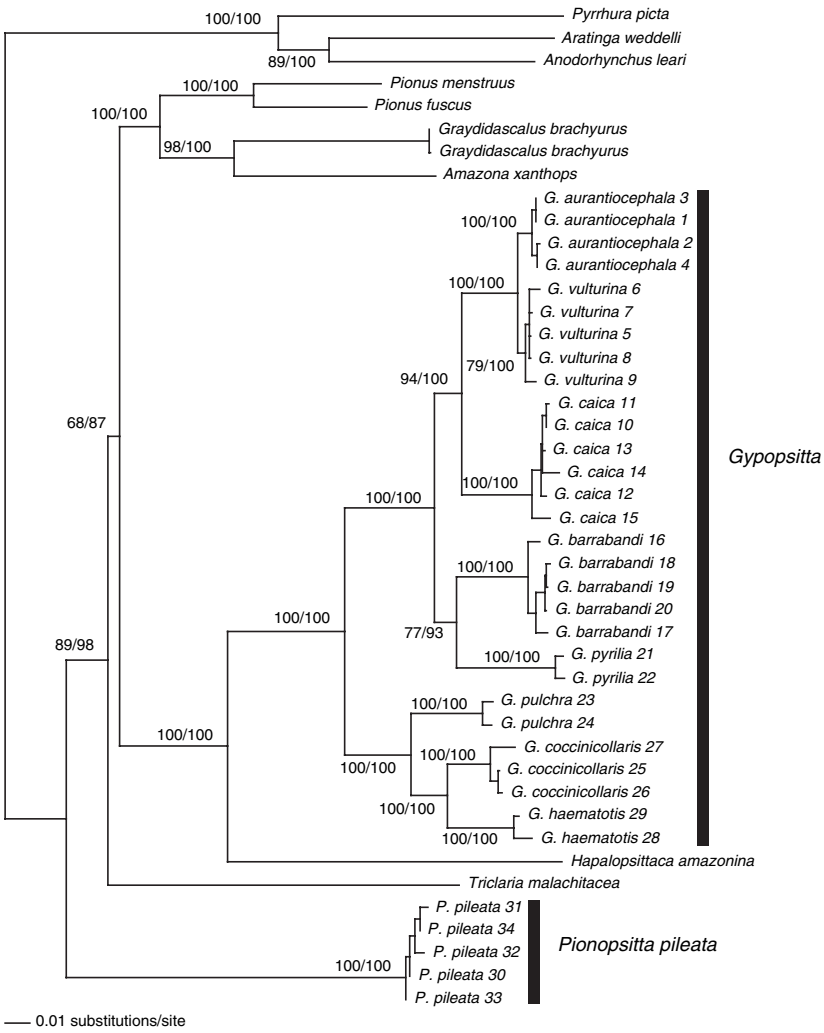

Figure 5 Maximum likelihood analysis of combined data (2181 bp): only topology found in PAUP. ML bootstrap values (100 replications) and Bayesian posterior probabilities, respectively, are shown on nodes.

Fig. 6. This pattern of relationships differs from the one found by Cracraft & Prum (1988) in that *G. barrabandi* was found to be the sister group to *G. pyrilia* instead of *G. vulturina* (compare Figs 2 & 6), but *G. caica* remains as the basal species of the Amazonian clade. Both morphological topologies (Figs 2 & 6) differ from the molecular results, in which *G. caica* appears as the sister group to *G. vulturina* and *G. aurantiocephala* (Figs 4 & 5).

Combined analysis

In order to investigate the phylogenetic position of *G. caica* further, we undertook a combined analysis. The morphological characters for all *Gypopsitta* species as well as for *H. amazonina* were added to the molecular data, thus creating a matrix of 2207 characters for 30 terminals. An MP analysis of these data (not shown) resulted in three most-parsimonious trees of 951 steps (consistency index excluding uninformative characters = 0.627), with the trees only differing by rearrangements among individuals of the same species. All three trees recovered *G. caica* as the sister group of [(*barrabandi* + *pyrilia*) + (*vulturina* + *aurantiocephala*)], a topology like that for morphology alone (also as in Cracraft & Prum, 1988). In the molecular analyses, *G. caica* grouped with *G. vulturina* and *G. aurantiocephala* with moderate to strong support (Figs 4 & 5), whereas with morphological data *G. caica* was the sister group of the Amazonian taxa with strong support (Fig. 6). In the combined analysis, *G. caica* is the sister group to the other Amazonian taxa with very weak support (< 50% bootstrap for 1000 replicates). Although the relationships found by the molecular data have moderate to strong support, it required only a few conflicting morphological characters to move *G. caica* to a basal position within the Amazonian clade.

Parametric bootstrap tests were used to test if the molecular data set rejected the topology found in the morphological analysis. Both the parametric test based on MP and the Shimodaira–Hasegawa test did not reject the null hypothesis (the morphological topology) ($P > 0.05$, Table 7), agreeing with the results found in the combined (molecular + morphology) analysis, thus suggesting uncertainty in both the molecular and morphological data regarding the position of *G. caica*. On the other hand, the likelihood-based SOWH test did reject the null hypothesis ($P < 0.001$, Table 7), thus showing that there is phylogenetic signal in the molecular data

Table 6 Morphological character matrix for 26 characters for eight *Gypopsitta* species and for the outgroup taxon, *Hapalopsittaca amazonina*

	Characters*																									
Taxa	1	2	3	4	5	6	7	8	9	10	11	12	13	14	15	16	17	18	19	20	21	22	23	24	25	26
H. amazonina	1	0	1	1	0	0	0	0	0	0	0	0	0	0	0	0	0	0	0	0	1	0	0	1	0	0
G. coccinicollaris	0	0	0	1	0	1	0	0	0	1	1	0	0	0	0	1	2	0	0	0	1	0	0	1	1	1
G. haematotis	0	0	0	1	0	0	0	0	0	1	1	0	0	0	0	1	2	0	0	0	1	0	0	1	1	1
G. pulchra	0	0	0	1	0	0	0	0	0	1	1	0	0	0	0	1	1	0	1	0	1	0	0	1	0	0
G. barrabandi	1	1	1	0	1	0	1	1	0	1	0	1	0	0	0	0	0	1	0	1	0	1	1	0	0	0
G. vulturina	1	1	1	0	1	0	1	0	1	1	0	1	0	1	0	0	0	0	0	1	0	0	1	0	0	0
G. pyrilia	1	1	1	0	1	0	1	0	0	0	0	0	1	0	0	0	0	0	0	1	0	1	1	0	0	0
G. caica	0	0	0	1	0	0	1	0	0	1	0	1	0	0	1	0	0	0	0	1	0	0	1	0	0	0
G. aurantiocephala	1	1	1	0	1	0	1	0	1	1	0	1	0	0	0	0	0	0	0	1	0	0	1	0	0	0

*Characters and character states are defined as follows: (1) red pigmentation on the lesser wing coverts and leading edge of wing: 0 (absent), 1 (present); (2) bright red pigmentation on greater underwing coverts: 0 (absent), 1 (present); (3) shoulder patch with distinct yellow/red/orange (carotenoid) pigmentation: 0 (absent), 1 (present); (4) upper breast dark red-tinged brownish-green: 0 (absent), 1 (present); (5) upper breast light yellowish-green: 0 (absent), 1 (present); (6) red on upper breast: 0 (absent), 1 (present); (7) belly with iridescent blue sheen to green feathers: 0 (absent), 1 (present); (8) tibial feathering with extensive yellow or orange: 0 (absent), 1 (present); (9) head feathers reduced on anterior portion of crown: 0 (absent), 1 (present); (10) forehead, crown, and nape moderately to heavily melanized: 0 (absent), 1 (present); (11) forehead, crown, and nape dark grey-green: 0 (absent), 1 (present); (12) crown and nape black: 0 (absent), 1 (present); (13) crown, nape and hindneck yellow: 0 (absent), 1 (present); (14) yellow collar on hindneck: 0 (absent), 1 (present); (15) ill-defined yellow-orange band at juncture of neck and back: 0 (absent), 1 (present); (16) red on auriculars: 0 (absent), 1 (present); (17) size of red patch on auriculars (character 16): 0 (absent, inapplicable), 1 (large), 2 (small); (18) deep yellow-orange malar patches: 0 (absent), 1 (present); (19) face extensively pinkish-red: 0 (absent), 1 (present); (20) basal portion of inner web of tail yellow (ventral view): 0 (absent), 1 (present); (21) red on inner web of tail (ventral view): 0 (absent), 1 (present); (22) lores only partly feathered: 0 (absent), 1 (present); (23) trailing edge of primaries green (ventral view): 0 (absent), 1 (present); (24) trailing edge of primaries blue or blue-green (ventral view): 0 (absent), 1 (present); (25) crown and nape dark olive in tone, forming well-defined border posteriorly with green of upper back: 0 (absent), 1 (present); (26) malar and throat dark greyish: 0 (absent), 1 (present).

that conflicts with the morphological data regarding the position of *G. caica*.

Molecular clock

For the molecular clock analyses, matrices containing only *Gypopsitta* species and *H. amazonina* were constructed (30 terminals). The likelihood ratio test showed that there was no significant difference between the $-\ln L$ values for the unconstrained cyt *b* ML tree (3803.1933) vs. the clock-enforced tree (3819.4637) ($P > 0.30$), but did show significant differences for the ND2 and combined data sets, and thus only cyt *b* data will be used here for inference of divergence times. The branch length and two cluster tests implemented in Lintree (Takezaki *et al.*, 1995) indicated no relative rate differences among the sequences included in the cyt *b* matrix.

The branch lengths of the ML tree constructed using the parameters chosen by MODELTEST for the corresponding matrix (TrN + Γ, $\alpha = 0.1747$) were used to estimate the divergence times. Two estimates of rates of cyt *b* sequence evolution (1.6% Myr^{-1}, Fleischer *et al.*, 1998; 2.0% Myr^{-1}, Shields & Wilson, 1987; Randi, 1996) were applied in order to encompass the range of rates reported for the gene. From these, two divergence dates and standard errors (corresponding to the errors associated with the distance measures) were obtained for each node (Fig. 7).

DISCUSSION

Saturation analyses and comparative utility of mtDNA genes for phylogenetic reconstruction

Both genes showed signs of saturation at third positions when the pairwise comparisons included outgroups (outside *Gypopsitta*). As reported for other groups of birds (Griffiths, 1997), cyt *b* sequences become saturated at distances above 9% divergence. Variable sites were more concentrated at third positions in cyt *b* sequences (69.2% of the variable sites for the complete matrix) than in ND2 sequences (56.7%). ND2 was more variable in general: this gene has also been found to be more variable than cyt *b* in other groups of birds (Hackett, 1996) and this is related, in our data set, to a greater accumulation of substitutions in first and second positions in ND2.

In their study of waterfowl Johnson & Sorenson (1998) concluded that ND2 and cyt *b* evolve at similar rates if the time since divergence has been relatively recent, and that a large part of their sequence evolution is governed by base composition bias and transition/transversion bias. They also found that the transition/transversion bias was similar in the two genes. In these parrots we found differences in rates of evolution (Fig. 3) and in transition/transversion rates (Table 3). These results may be due to greater evolutionary divergence among the sequences studied here, but may also

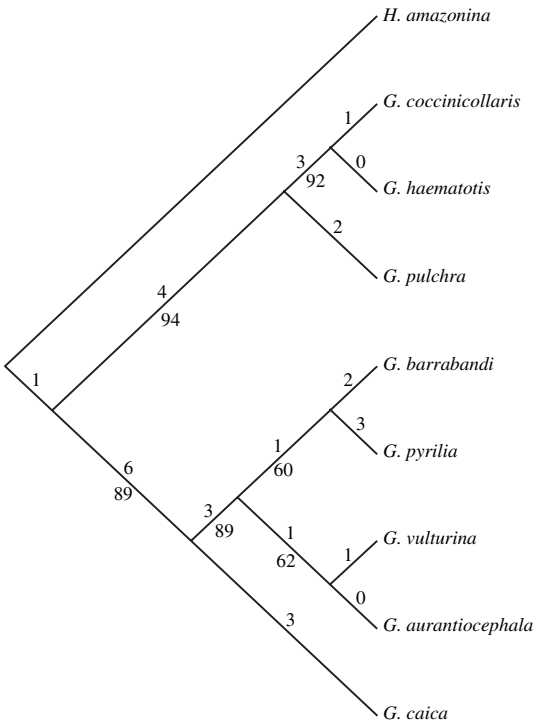

Figure 6 Topology resulting from the MP analysis of the revised morphological matrix, containing 26 plumage characters. The tree has 32 steps. The number of character changes supporting each node is shown above branches, bootstrap support values are shown below branches.

be an indication that these two protein-coding genes present some differences in their patterns of sequence evolution and thus may have different utilities in reconstructing phylogenies.

Molecular systematics

The phylogenetic results strongly confirm that the genus conventionally recognized as *Pionopsitta* is not monophyletic. The type species of the genus, *P. pileata*, does not group with the other species traditionally included in the genus and instead is separated from them by at least two branching events. Our results strongly identify *H. amazonina* as the sister group to *Gypopsitta*. Lying outside these taxa, moreover, is a well-supported clade containing the genera *Pionus*, *Graydidascalus* and *Amazona xanthops*, a relationship found independently by Russello & Amato (2004). Together, *Pionus*, *Graydidascalus* and *Amazona xanthops* are resolved as the sister group of *H. amazonina* + *Gypopsitta*, but the branch support for this relationship is low. *Triclaria malachitacea* appears as sister group to *P. pileata* in unweighted MP analyses with medium support (69%, see Fig. 4) but in the ML analysis *P. pileata* lies outside *T. malachitacea* and the other taxa (Fig. 5).

Relationships among species

In our analyses, mtDNA haplotypes in the ingroup revealed seven clearly defined clusters, supported by high bootstrap values (79–100%), that correspond to six of the seven species recognized by Cracraft & Prum (1988). The seventh species, *G. aurantiocephala*, was only described recently and appears as the sister species to *G. vulturina*. Both *G. vulturina* and *G. aurantiocephala* individuals are reciprocally monophyletic in all analyses. These results provide additional strong support for the validity of the new species as well as for its relationship to *G. vulturina*. The phylogeny also reveals that *cis*/*trans* Andean clades represent monophyletic groups, as postulated by Cracraft & Prum (1988), and both these clades have high support.

In both MP and ML analyses (Figs 4 & 5) *G. vulturina* and *G. aurantiocephala* were found to be sister to *G. caica* with moderate to strong support, and *G. pyrilia* and *G. barrabandi* were moderately supported as sister taxa. This arrangement contradicts the phylogeny proposed by Cracraft & Prum (1988) in which *G. vulturina* is sister to *G. barrabandi*, *G. pyrilla* is their sister group, and *G. caica* has a basal position (Fig. 2). In the Cracraft and Prum analysis, the *G. barrabandi* + *G. vulturina* clade was supported by five exclusive characters and one parallelism shared with *G. caica*. The reanalysis of the morphological data presented here recovers a clade composed of [(*G. barrabandi*, *G. pyrilia*), (*G. vulturina*, *G. aurantiocephala*)], with *G. caica* appearing as their sister group (Fig. 6). Although this arrangement has strong support in the morphological data, and is also recovered in the combined analysis, the basal position of *P. caica* has extremely weak support in this last analysis (see Results).

The mtDNA phylogeny is well-resolved and nearly all nodes are strongly supported. Thus, assuming that *G. caica* is the sister group to (*G. vulturina*, *G. aurantiocephala*), its basal position in the morphological and combined trees could be explained either by its having retained multiple ancestral character states or by having regained them, depending on how character changes are optimized. In either case *G. caica* would have the primitive condition for these characters relative to the other four species. Although we judge the molecular topology to be our best estimate of relationships, additional data will be required to resolve *G. caica*'s position more completely.

Table 7 Tests of the null hypothesis (H_0) of the topology resulting from the morphological analyses

Test	Critical value for difference at 5% confidence level	Observed difference	*P*-value	Rejection of H_0
SOWH (ML)	0.97	9.59	< 0.001	Yes
Parametric bootstrap (MP)	3.2	2.0	> 0.05	No
Shimodaira–Hasegawa (ML)	–	9.90	0.075	No

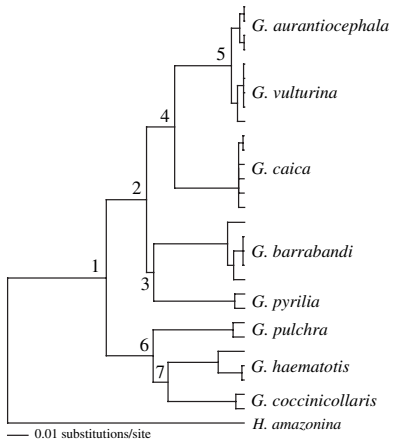

Node	Geographical separation	ML distance (%)	Date 2.0% (Ma)	Date 1.6% (Ma)
1	Cis/trans Andes	13.91 ± 0.21	6.95 (6.84–7.06)	8.69 (8.56–8.82)
2	E/W Amazonia	10.18 ± 0.19	5.09 (4.99–5.19)	6.36 (6.24–6.48)
3	W Amazonia/NW Venezuela	9.86 ± 0.59	4.93 (4.63–5.23)	6.16 (5.79–6.53)
4	Guianas/Pará	6.66 ± 0.18	3.33 (3.24–3.42)	4.16 (4.05–4.27)
5	Belém-Pará/Rondônia	1.14 ± 0.08	0.57 (0.53–0.61)	0.71 (0.66–0.76)
6	Chocó/Central America	9.32 ± 0.57	4.66 (4.38–4.94)	5.83 (5.47–6.19)
7	N/SCentral America	7.86 ± 0.62	3.93 (3.62–4.24)	4.91 (4.52–5.30)

Figure 7 Maximum likelihood analysis of cyt *b* data for the ingroup only, with the molecular clock enforced. The accompanying table shows, for each node, the geographical disjunction, the corresponding distance with standard error, and the estimated divergence dates using the rates of 2.0% and 1.6% divergence Myr^{-1}. The minimum and maximum estimated age of divergence for each node (in parentheses) were calculated based on the standard error for the distance measure associated with that node.

Genetic distances and species limits

The genetic distance between *G. vulturina* and *G. aurantiocephala* was significantly smaller than the distances among the other species (1.0% in cyt *b* and 1.5% in ND2). Nevertheless, the existence of diagnostic morphological (Gaban-Lima *et al.*, 2002) and molecular characters (see Results) supports their recognition as different species under the Phylogenetic Species Concept *sensu* Cracraft (1983), Nixon & Wheeler (1990) and Davis & Nixon (1992). Better sampling will be needed to refine distributional limits of these species and confirm the absence of intermediate forms in nature.

Gypopsitta coccinicollaris has been considered a subspecies of *G. haematotis* by some authors (Haffer, 1970; Forshaw, 1989), while Cracraft & Prum (1988) consider these two taxa as separate species. These species occur in southern and northern Central America and there seems to exist a region of sympatry in Panama. In the present study, one of the sampled *G. coccinicollaris* individuals (number 27) is from a locality that is closer to those of the two *G. haematotis* specimens from Veraguas than it is to the other two *G. coccinicollaris* collected in Darien Province (see Fig. 1). Despite the geographical proximity and phenotypic similarity between these two species, interspecific distances were markedly higher (2.6% in ND2, 4.6% in cyt *b*) than the intraspecific distances (0.1–1.2%), indicating the existence of an effective barrier separating these two species in the past.

Spatial and temporal patterns of diversification of *Gypopsitta*: testing biogeographical hypotheses

The biogeographical interpretations discussed below are based on the molecular phylogenetic results as well as on the range of divergence times estimated from the ML analysis and molecular clock calculations (Fig. 7). Drawing correlations, let alone causal relationships, between biogeographical patterns such as area relationships, on the one hand, and Earth history, on the other, is difficult. Events of Earth history that result in vicariance, such as mountain uplift or the initiation of river barriers, generally are established over long periods of time (relative to taxonomic differentiation) and determining when those geological changes might be sufficient to isolate populations of organisms will often be uncertain. Likewise, a description of the biogeographical history of a single group, such as the parrots discussed here, cannot lead by itself to biogeographical generalizations without comparison to other groups (Nelson & Platnick, 1980). Consequently inferences about common causation, such as vicariance events, are limited.

Cis/trans (east/west) Andean disjunction

The two major lineages of *Gypopsitta* are distributed on opposite sides of the Andes (Fig. 1), with the west Andean *haematotis* species group occurring from the Chocó area of endemism in Colombia, through Central America to southern Mexico, whereas the remaining species are distributed within Amazonia and northern South America. For decades investigators have recognized a small number of explanations to account for taxonomically differentiated disjuncts west of the Andean mountains (e.g. Chapman, 1917; Haffer, 1967, 1974; Cracraft & Prum, 1988; Brumfield & Capparella, 1996). The first hypothesis proposes that the *trans*-Andean avifauna originated from populations distributed throughout an ancestral northern Amazonian-Pacific lowland forest that was subsequently fragmented by Andean uplift. Thus, the

Andean uplift hypothesis has generally made the prediction that the divergence dates between these groups should be roughly coincident in time with, or slightly younger than, the main uplift of the Andean Cordillera (but see below).

Haffer (1967, 1974, pp. 159–161) championed a second hypothesis, namely that the Chocó avifauna resulted from the expansion of Amazonian populations into north-western Colombia and the Chocó during Pleistocene humid periods and were then isolated in a wet Chocó 'refuge' during drier interglacial periods. Although the *forest refugia hypothesis* makes no direct prediction about the dates of divergence among species – refuge formation is assumed to have been possible at multiple times (and not only during the Pleistocene; see Haffer, 1993) – it has been most commonly interpreted as applying to periods of high amplitude cyclical climate change in the Pleistocene. The refuge hypothesis, moreover, assumes that mountain uplift was not the primary barrier causing disjunction (Haffer, 1967, 1974) and that climatic/ecological vicariance would have taken place *after* mountain building (e.g. Haffer, 1967; Brumfield & Capparella, 1996, p. 1611). Adopting these assumptions, however, does not allow for a critical test of the two hypotheses, inasmuch as isolation by climatic fluctuation could be invoked either before or after mountain uplift.

The northern Andes are divided into three ranges with different tectonic histories: the Western, Central, and the Eastern Cordillera and its adjacent ranges. The Western Cordillera is formed from accretion of oceanic terranes (volcanic island arc) that were emplaced from the Early Cretaceous into the Cenozoic (Case *et al.*, 1990), and to the west, the Chocó block was accreted to South America beginning in the Middle Miocene (Duque-Caro, 1990). As a consequence, the region experienced significant uplift from Miocene to Holocene times (Case *et al.*, 1990).

The Central and Eastern Cordilleras are mostly underlain by continental crust (Case *et al.*, 1990). The Central Cordillera is the older of the two and had its initial uplift in the Late Cretaceous into the Paleogene (Gómez *et al.*, 2003), apparently in response to accretion of terranes to the west (Cooper *et al.*, 1995). Uplift of the Eastern Cordillera began approximately at 12.9 Ma, and a continuous mountain range, probably low-lying, was created by 11.8 Ma since westward sediment-fill into the Magdalena Valley indicates increased elevation (Hoorn *et al.*, 1995; Guerrero, 1997). This onset of uplift appears causally related to the accretion of the Chocó terrain to the Western Cordillera, beginning *c.* 12 Ma (Duque-Caro, 1990; Dengo & Covey, 1993; Cooper *et al.*, 1995), which resulted in compression across the Colombian Andes. To the north and west, the Santander massif followed an uplift history similar to that of the Eastern Cordillera (Hoorn *et al.*, 1995; Gregory-Wodzicki, 2000), but it and the Sierra de Perijá, the Santa Marta massif, and the Mérida Andes experienced their main uplift in the Late Miocene–Pliocene (Kellogg, 1984; Hoorn *et al.*, 1995).

Within this broad geological context, how might the history of *Gypopsitta* and other *cis*/*trans* Andean disjuncts be interpreted? Using the standard error estimates for our molecular clock dates, the separation between the east and west Andean clades of *Gypopsitta* (Fig. 7, node 1) occurred between 8.82 and 6.84 Ma, during the Late Miocene. This age is more consistent with vicariance resulting from Andean uplift (Eastern Cordillera) than with the traditional refuge hypothesis. At this time the Chocó terrane was being implaced, creating for the first time significant lowland habitat west of the Western Cordillera (Duque-Caro, 1990). It seems unlikely that vicariance of these disjuncts would have been created by Western or Central Cordilleran uplift, as these ranges were already in place and were being raised even further. In contrast, the north-eastern Andes, including the Eastern Cordillera, and probably also the Santander and Sierra de Perijá ranges, were relatively low in elevation prior to 8 Ma and experienced their greatest uplift after *c.* 5–6 Ma (Hoorn *et al.*, 1995; Gregory-Wodzicki, 2000; Hooghiemstra & Van der Hammen, 2004). This temporal history of uplift is consistent with our estimated age of divergence between the east and west Andean clades of *Gypopsitta*, but it does not completely explain the current distribution of *G. pulchra* in the Chocó.

The molecular data suggest that the three west Andean species of *Gypopsitta* are old and arose in the Early Pliocene or perhaps the latest part of the Late Miocene (Fig. 7, nodes 6 and 7). This was a time of high global temperatures, especially around a closing Panamanian Isthmus (Crowley, 1991), and regional temperature fluctuations during this period would have been less than at higher latitudes (Dowsett *et al.*, 1996). It is not likely, therefore, that climate oscillations were important for driving species formation at this time. Instead, sea-level fluctuations may have played a major role in subdividing lowland and lower-montane populations as Nores (2004) has previously suggested. Over the period of time that the *G. haematotis* species-group presumably was diversifying, beginning as early as 6.19 Ma (Fig. 7, node 6) until as late as 3.62 Ma (Fig. 7, node 7) there were at least three major episodes of sea-level rise and fall (Krantz, 1991) that probably would have been sufficient to isolate populations to the west in the Chocó and Nechí regions as well as to the north in Central America.

Finally, our results for the timing of the east vs. west Andean disjunction are very similar to those of Cortés-Ortiz *et al.* (2003) for howler monkeys (*Alouatta*) and for several lineages of curassows (Pereira & Baker, 2004). Using several mitochondrial genes, including cyt *b*, Cortés-Ortiz *et al.* (2003) estimated the *cis*/*trans* Andean disjunction at around 6.8 Ma. In contrast to our results (Fig. 7), differentiation within the Chocó-Central American monkey taxa began later, *c.* 3.0 Ma, but most of that took place within Central America. Any disjunction between Chocó and Central American populations of *A. palliata*, which was not investigated with their sampling, would have been still younger. The estimated ages of the *cis*/*trans* Andean disjunctions in both *Alouatta* and *Gypopsitta* are older than that postulated for *Bufo marinus* at 2.7 Ma (Slade &

Moritz, 1998). Likewise, Pereira & Baker (2004), using six mitochondrial regions, estimated the mean age of *cis*/*trans* Andean disjuncts in curassows to be *c.* 5.5–8.2 Ma. All of these ages, it should be noted, are older than the onset of Plio-Pleistocene glacial climates beginning *c.* 2.4 Ma.

Eastern Andean taxa: diversification in the Amazon basin

The previous analysis of *Gypopsitta* by Cracraft & Prum (1988) postulated a sequence of vicariant events that partitioned the species within Amazonia. Their first proposed vicariance event isolated the Guyanan centre of endemism, the second segregated south-eastern Amazon, and the last subdivided the western Amazon region (Cracraft & Prum, 1988). The molecular results obtained in this study point to a different order for these events, and the dates obtained from the molecular clock estimates suggest that much of the diversification in this group took place as early as Late Miocene and Pliocene times.

Using the molecular tree as a basis for inference, the first vicariance event within the east Andean species was an east/west break that separated the lineage leading to *G. barrabandi* and *G. pyrilia* from that of (*G. caica* [*G. vulturina*, *G. aurantiocephala*)]. Depending on the rate of molecular evolution in cytochrome *b* that is applied, this event is estimated to have occurred in the Late Miocene/Early Pliocene (between 6.48 and 4.99 Ma; Fig. 7, node 2). Moreover, except for the divergence of *G. aurantiocephala* and *G. vulturina* (see below), all speciation events in Amazonian *Gypopsitta* pre-date the Pleistocene. For the reasons articulated in our discussion about the west Andean species, it is also not likely that vicariance among the east Andean species was driven by cyclical climate change, although admittedly very little is known about Amazon basin climate and vegetation during the relevant time period. Sea-level fluctuations may have played a role (Nores, 1999), although it is not clear how those might have affected the biogeographical pattern exhibited by *Gypopsitta*. If *G. caica* and *G. vulturina*/*G. aurantiocephala* are related, as indicated by the molecular data (Fig. 7, node 4), then their distribution lies east of the Negro and Madeira rivers, whereas *G. barrabandi* + *G. pyrilia* are distributed to the west. The Amazon River system, however, apparently cut through the Purus and Monte Alegre arches to become transcontinental in the Late Miocene, perhaps as early as 11 Ma (Hoorn, 1994) or as late as 8.5–8.0 Ma (Lundberg *et al.*, 1988), too early, it would seem, to have directly caused divergences within *Gypopsitta*. It is possible, however, that later the evolving Amazon did play a role in the vicariance between *G. caica* and *G. vulturina*/*aurantiocephala*.

It seems likely that speciation of *G. pyrilia* and *G. barrabandi* (Fig. 7, node 3) are related to Pliocene tectonic events in northern Amazonia. Either mountain building or possibly marine transgressions could have partitioned off *G. pyrilia* from an ancestral population that extended south through western Amazonia. We estimate that event took place between 6.53 and 4.63 Ma, which as discussed earlier, is coincident with a period of major uplift in the Eastern Cordillera and associated ranges.

Thus, the evidence suggests that most speciation events in *Gypopsitta* can be related to palaeogeographical events that took place in South America before the Quaternary. The only divergence that occurred during the Quaternary was the *G. vulturina*/*G. aurantiocephala* split, between 0.76 and 0.53 Ma (Fig. 7, node 5). These two taxa currently exhibit distributions that are congruent with proposed areas of endemism (Belém/Pará area and between the Tapajós and Xingú rivers in the Rondônia area, respectively; Cracraft, 1985; Haffer, 1985), and they are sympatric along the middle and lower Tapajós and lower Madeira rivers (Gaban-Lima *et al.*, 2002). Glacial cycles may have had an influence on this speciation event, but the fine-grained evidence to test this is currently lacking.

ACKNOWLEDGEMENTS

A.L. Porzecanski, P. Brito and G. Marroig are gratefully acknowledged for discussions about specific topics. R. Teixeira and L. F. Silveira were of great help in providing some of the samples used. Two anonymous referees provided valuable suggestions. We thank Donna Dittman and Fred Sheldon for providing tissue from the Genetic Resources Collection, Louisiana State University Museum of Natural Science; David Willard and Shannon Hackett for providing tissues from the Field Museum of Natural History; James Dean and Mike Braun for providing tissues from the National Museum of Natural History; Mark Robbins for providing tissues from the Kansas University Natural History Museum; Maria Luiza Marceliano for providing tissue from the Museu Paraense Emílio Goeldi; Leo Joseph for providing tissues from the Academy of Natural Sciences; P. Sweet for assistance with skin samples from the American Museum of Natural History. P. Sweet provided collection locality data from the AMNH specimens. J. Feinstein, P. Brito and J. Groth kindly provided the sequences of some of the primers used. This work was supported by Fundação de Amparo à Pesquisa do Estado de São Paulo, Coordenação de Aperfeiçoamento de Pessoal de Nível Superior, and Conselho Nacional de Pesquisa. This paper is a contribution from the Monell Molecular Laboratory and the Cullman Research Facility in the Department of Ornithology, American Museum of Natural History, and has received generous support from the Lewis B. and Dorothy Cullman Program for Molecular Systematics Studies, a joint initiative of The New York Botanical Garden and The American Museum of Natural History.

REFERENCES

Aleixo, A. (2002) Molecular systematics and the role of the 'Várzea'-'Terra Firme' ecotone in the diversification of *Xiphorhynchus* woodcreepers (Aves; Dendrocolaptidae). *Auk*, **119,** 621–640.

Aleixo, A. (2004) Historical diversification of a Terra-firme forest bird superspecies: a phylogeographic perspective on the role of different hypotheses of Amazonian diversification. *Evolution*, **38,** 1303–1317.

Bates, J., Hackett, S. & Cracraft, J. (1998) Area-relationships in the Neotropical lowlands: an hypothesis based on raw distributions of Passerine birds. *Journal of Biogeography*, **25,** 783–793.

Bremer, K. (1994) Branch support and tree stability. *Cladistics*, **10,** 295–304.

Brumfield, R.T. & Capparella, A.P. (1996) Historical diversification of birds in northwestern South America: a molecular perspective on the role of vicariant events. *Evolution*, **50,** 1607–1624.

Burns, K.J. & Naoki, K. (2004) Molecular phylogenetics and biogeography of Neotropical tanagers in the genus *Tangara*. *Molecular Phylogenetics and Evolution*, **32,** 838–854.

Bush, M.B. (1994) Amazonian speciation: a necessarily complex model. *Journal of Biogeography*, **21,** 5–17.

Case, J.E., Shagam, R. & Giegengack, R.F. (1990) Geology of the northern Andes; an overview. *The geology of North America. Vol. H. The Caribbean region* (ed. by G. Dengo and J.E. Case), pp. 177–200. Geological Society of America, Boulder, CO.

Chapman, F.M. (1917) The distribution of bird life in Colombia. *Bulletin of the American Museum of Natural History*, **36,** 1–729.

Cheng, S., Higuchi, R. & Stoneking, M. (1994) Complete mitochondrial genome amplification. *Nature Genetics*, **7,** 350–351.

Cooper, M.A., Addison, F.T., Alvarez, R., Coral, M., Graham, R.H., Hayward, A.B., Howe, S., Martinez, J., Naar, J., Peñas, R., Pulham, A.J. & Taborda, A. (1995) Basin development and tectonic history of the Llano basin, Eastern Cordillera and middle Magdalena valley, Colombia. *American Association of Petroleum Geologists Bulletin*, **79,** 1421–1443.

Cortés-Ortiz, L., Bermingham, E., Rico, C., Rodríguez-Luna, E., Sampaio & I., Ruiz-Garcia, M. (2003) Molecular systematics and biogeography of the Neotropical monkey genus *Alouatta*. *Molecular Phylogenetics and Evolution*, **26,** 64–81.

Costa, L. (2003) The historical bridge between the Amazon and the Atlantic Forest of Brazil: a study of molecular phylogeography with small mammals. *Journal of Biogeography*, **30,** 71–86.

Cracraft, J. (1983) Species concepts and speciation analysis. *Current Ornithology*, **1,** 159–187.

Cracraft, J. (1985) Historical biogeography and patterns of differentiation within the South American avifauna: areas of endemism. *Ornithological Monographies*, **36,** 49–84.

Cracraft, J. (1988) Species as entities of biological theory. pp. 31–52. *What the philosophy of biology is* (ed. by M. Ruse). D. Reidel, Dordrecht. 321 p.

Cracraft, J. & Prum, R.O. (1988) Patterns and processes of diversification: speciation and historical congruence in some neotropical birds. *Evolution*, **42,** 603–620.

Crowley, T.J. (1991) Modeling Pliocene warmth. *Quaternary Science Reviews*, **10,** 275–282.

Davis, J.I. & Nixon, K.C. (1992) Populations, genetic variation and the delimitation of phylogenetic species. *Systematic Biology*, **41,** 421–435.

Dengo, C.A. & Covey, M.C. (1993) Structure of the eastern Cordillera of Colombia: implications for trap styles and regional tectonics. *American Association of Petroleum Geologists Bulletin*, **77,** 1315–1337.

Dowsett, H., Barron, E.J. & Poore, R.Z. (1996) Middle Pliocene seasurface temperatures: a global reconstruction. *Marine Micropaleontology*, **27,** 13–25.

Duque-Caro, H. (1990) The Chocó block in the northwestern corner of South America: structural, tectonostratigraphic, and paleogeographic implications. *Journal of South American Earth Sciences*, **3,** 71–84.

Endler, J.A. (1977) *Geographic variation, speciation and clines*. Princeton University Press, Princeton, NJ.

Eriksson, T. (1999) *AutoDecay ver. 4.0 (program distributed by the author)*. Bergius Foundation, Royal Swedish Academy of Sciences, Stockholm.

Farris, J.S., Kallersjo, M., Kluge, A.G. & Bult, C. (1995) Testing significance of incongruence. *Cladistics*, **10,** 315–319.

Fleischer, R.C., Mcintosh, C.E., Tarr, C.L. (1998) Evolution on a volcanic conveyor belt: using phylogeographic reconstructions and K–Ar-based ages of the Hawaiian Islands to estimate molecular evolutionary rates. *Molecular Ecology*, **7,** 533–545.

Forshaw, J. (1989) *Parrots of the world*. Third (revised) Edition. Landsdowne Editions. Illustrated by W. Cooper. pp. 672, Melbourne, Australia.

Gaban-Lima, R., Raposo, M. & Höfling, E. (2002) Description of a new species of *Pionopsitta* (Aves, Psittacidae) endemic to Brazil. *Auk*, **119,** 815–819.

Goldman, N., Anderson, J.P. & Rodrigo, A.G. (2000) Likelihood-based tests of topologies in phylogenetics. *Systematic Biology*, **49,** 652–676.

Gómez, E., Jordan, T.E., Allmendinger, R.W., Hegarty, K., Kelley, S. & Heizler, M. (2003) Controls on architecture of the Late Cretaceous to Cenozoic Southern Middle Magdalena valley basin, Colombia. *GSA Bulletin*, **115,** 131–147.

Gregory-Wodzicki, K.M. (2000) Uplift history of the central and northern Andes: a review. *GSA Bulletin*, **112,** 1091–1105.

Griffiths, C.S. (1997) Correlation of functional domains and rates of nucleotide substitution in cytochrome *b*. *Molecular Phylogenetics and Evolution*, **7,** 352–365.

Guerrero, J. (1997) Stratigraphy, sedimentary environments, and the Miocene uplift of the Colombian Andes. *Vertebrate paleontology in the neotropics: the Miocene fauna of La Venta, Colombia* (ed. by R.F. Kay, R.H. Madden, R.L. Cifelli and J.J. Flynn), pp. 15–43. Smithsonian Institution Press, Washington, DC.

Hackett, S. (1996) Molecular phylogenetics and biogeography of tanagers in the genus *Ramphocelus*. *Molecular Phylogenetics and Evolution*, **5,** 368–382.

Haffer, J. (1967) Speciation in Colombian forest birds west of the Andes. *American Museum Novitates*, **294,** 1–57.

Haffer, J. (1969) Speciation in Amazonian forest birds. *Science*, **165,** 131–137.

Haffer, J. (1970) Art-Entstehung bei einigen Waldvögeln Amazoniens. *Journal of Ornithology*, **111,** 285–331.

Haffer, J. (1974) *Avian speciation in tropical South America*. Nuttall Ornithological Club, Cambridge, MA.

Haffer, J. (1985) Avian zoogeography of the neotropical lowlands. *Ornithological Monographs*, **36,** 113–146.

Haffer, J. (1993) Time's cycle and time's arrow in the history of Amazonia. *Biogeographica*, **69,** 15–45.

Haffer, J. (1997) Alternative models of vertebrate speciation in Amazonia: an overview. *Biodiversity Conservation*, **6,** 451–477.

Hooghiemstra, H. & Van der Hammen, T. (2004) Quaternary ice-age dynamics in the Colombian Andes: developing an understanding of our legacy. *Philosophical Transactions of the Royal Society*, **359B,** 173–181.

Hoorn, C. (1994) An environmental reconstruction of the palaeo-Amazon River system (Middle-Late Miocene, NW Amazonia). *Palaeogeography, Palaeoclimatology, Palaeoecology*, **112,** 187–238.

Hoorn, C., Guerrero, J., Sarmiento, G.A., Lorente, M.A. (1995) Andean tectonics as a cause for changing drainage patterns in Miocene northern South America. *Geology*, **23,** 237–240.

Huelsenbeck, J.P. & Rannala, B. (1997) Phylogenetic methods come of age: testing hypotheses in an evolutionary context. *Science*, **276,** 227–232.

Huelsenbeck, J.P. & Ronquist, F. (2001) MRBAYES: Bayesian inference of phylogeny. *Bioinformatics*, **17,** 754–755.

Huelsenbeck, J.P., Hillis, D.M. & Jones, R. (1996) Parametric bootstrapping in molecular phylogenetics: applications and performances. *Molecular zoology: advances, strategies, and protocols* (ed. by J.D. Ferraris and S.R. Palumbi), pp. 19–45. Wiley-Liss, New York.

Johnson, K.P. & Sorenson, M.D. (1998) Comparing molecular evolution in two mitochondrial protein coding genes (cytochrome b and ND2) in the dabbling ducks (Tribe: Anatini). *Molecular Phylogenetics and Evolution*, **10,** 82–94.

Kellogg, J.N. (1984) Cenozoic tectonic history of the Sierra de Perijá, Venezuela-Colombia, and adjacent basins. *Geological Society of America Memoirs*, **162,** 239–261.

Kishino, H. & Hasegawa, M. (1989) Evaluation of the maximum likelihood estimate of the evolutionary tree topologies from DNA sequence data, and the branching order in Hominoidea. *Journal of Molecular Evolution*, **29,** 170–179.

Krantz, D.E. (1991) A chronology of Pliocene sea-level fluctuations: the U.S. middle Atlantic coastal plain record. *Quaternary Science Reviews*, **10,** 163–174.

Kumar, S., Tamura, K. & Nei, M. (2001) *MEGA: molecular evolutionary genetics analysis*. The Pennsylvania State University, Pennsylvania.

Maddison, W.P. & Maddison, D.R. (1999) *MacClade: analysis of phylogeny and character evolution*. Sinauer Associates, Sunderland, MA.

Marks, B.D., Hackett, S. & Capparella, A. (2002) Historical relationships among neotropical lowland forest areas of endemism as determined by mitochondrial DNA sequence variation within the Wedge-billed Woodcreeper (Aves: Dendrocolaptidae: *Glyphorhynchus spirurus*. *Molecular Phylogenetics and Evolution*, **24,** 153–167.

Miyaki, C.Y., Matioli, S., Burke, T & Wajntal, A. (1998) Parrot evolution and paleogeographic events: mitochondrial DNA evidences. *Molecular Biology and Evolution*, **15,** 544–551.

Nei, M. (1987) *Molecular evolutionary genetics*. Columbia University Press, New York.

Nelson, G. & Platnick, N. 1980. A vicariance approach to historical biogeography. *Bioscience*, **30,** 339–343.

Nixon, K.C. & Wheeler, Q.D. (1990) An amplification of the phylogenetic species concept. *Cladistics*, **6,** 211–223.

Nores, M. (1999) An alternative hypothesis for the origin of Amazonian bird diversity. *Journal of Biogeography*, **26,** 475–485.

Nores, M. (2004) The implications of Tertiary and Quaternary sea level rise events for avian distribution patterns in the lowlands of northern South America. *Global Ecology and Biogeography*, **13,** 149–161.

Patton, J.L., Silva, M.N.F. & Malcolm, J.R. (1994) Gene genealogy and differentiation among arboreal spiny rats (Rodentia: Echimydae) of the Amazon basin: a test of the riverine barrier hypothesis. *Evolution*, **48,** 1314–1323.

Pereira, S.L. & Baker, A.J. 2004. Vicariant speciation of curassows (Aves, Cracidae): a hypothesis based on mitochondrial DNA phylogeny. *Auk*, **121,** 682–694.

Platnick, N.I. & Nelson, G.J. (1978) A method of analysis for historical biogeography. *Systematic Zoology*, **27,** 1–16.

Posada, D. & Crandall, K.A. (1998) Modeltest: testing the model of DNA substitution. *Bioinformatics*, **14,** 817–818.

Quinn, T.W. (1997) Molecular evolution of the mitochondrial genome. *Avian molecular evolution and systematics* (ed. by D.P. Mindell), pp. 3–28. Academic Press, San Diego, CA.

Rambaut, A. & Grassly, N.C. (1997) Seq-Gen: an application for the Monte Carlo simulation of DNA sequence evolution along phylogenetic trees. *Computer Applications in Biosciences*, **1,** 235–238.

Randi, E. (1996) A mitochondrial cytochrome b phylogeny of the *Alectoris* partridges. *Molecular Phylogenetics and Evolution*, **6,** 214–227.

Ribas, C.C. & Miyaki, C.Y. (2004) Molecular systematics in *Aratinga* parakeets: species limits and historical biogeography in the '*solstitialis*' group and the systematic position of *Nandayus nenday*. *Molecular Phylogenetics and Evolution*, **30,** 663–675.

Ron, S.R. (2000) Biogeographic area-relationships of lowland Neotropical rain forest based on raw distributions of vertebrate groups. *Biological Journal of the Linnean Society*, **71,** 379–402.

Russello, M.A. & Amato, G. (2004) A molecular phylogeny of Amazona: implications for Neotropical parrot biogeography, taxonomy and conservation. *Molecular Phylogenetics and Evolution*, **30,** 421–37.

Salo, J., Kalliola, R., Hakkinen, L., Kakinen, Y., Niemela, P., Puhakka, M. & Coley, P.D. (1986) River dynamics and the diversity of Amazon lowland rain forest. *Nature*, **322,** 254–258.

Shields, G.F. & Wilson, A.C. (1987) Calibration of mitochondrial DNA evolution in geese. *Journal of Molecular Evolution*, **24,** 212–217.

Shimodaira, H. & Hasegawa, M. (1999) Multiple comparisons of log likelihoods with applications to phylogenetic inference. *Molecular Biology and Evolution*, **16,** 1114–1116.

Slade, R.W. & Moritz, C. (1998) Phylogeography of *Bufo marinus* from its natural and introduced ranges. *Proceedings of the Royal Society London*, **265B,** 769–777.

Sorenson, M.D., Ast, J.C., Dincheff, D.E., Yuri, T. & Mindell, D.P. (1999) Primers for a PCR-based approach to mitochondrial genome sequencing in birds and other vertebrates. *Molecular Phylogenetics and Evolution*, **12,** 105–114.

Swofford, D.L. (1998) PAUP*. Phylogenetic analysis using parsimony (*and other methods). Sinauer Associates, Sunderland, MA.

Takezaki, N., Rzhetski, A. & Nei, M. (1995) Phylogenetic test of the molecular clock and linearized trees. *Molecular Biology and Evolution*, **12,** 823–833.

Tavares, E.S., Yamashita, C. & Miyaki, C.Y. (2004) Phylogenetic relationships among some Neotropical parrot genera (Psittacidae; Aves) based on mitochondrial sequences. *Auk*, **121,** 230–242.

Templeton, A.R. (1983) Phylogenetic inference from restriction endonuclease cleavage site maps, with particular reference to the evolution of humans and the apes. *Evolution*, **37,** 221–244.

Tuomisto, H., Ruokolainen, K., Kalliola, R., Linna, A. & Danjoy, W., Rodrigues, Z. (1995) Dissecting Amazonian biodiversity. *Science*, **269,** 63–66.

Wallace, A.R. (1852) On the monkeys of the Amazon. *Proceedings of the Zoological Society London*, **20,** 107–110.

BIOSKETCHES

Camila C. Ribas received her PhD from Universidade de Sao Paulo. She is currently a Postdoctoral Fellow at the Department of Ornithology, American Museum of Natural History. Her research interests include historical biogeography of the Neotropical region, molecular systematics and patterns of diversification.

Renato Gaban-Lima is a doctoral candidate at the Zoology Department at the Universidade de Sao Paulo. His research focuses on morphology, systematics and biogeography of parrots.

Cristina Y. Miyaki is Associate Professor at the Biology Department at the Universidade de Sao Paulo. Her research focuses on molecular systematics, biogeography and phylogeography of birds.

Joel Cracraft is Lamont Curator of Birds and Curator-in-Charge, Department of Ornithology, American Museum of Natural History in New York. His research interests include avian systematics, historical biogeography and biological diversification.

Editor: Robert Whittaker